SUSTAINABLE DEVELOPMENT
OF FLOODPLAIN TERRITORIES OF REGULATED RIVERS.
PART I: Modeling Complex Structure Dynamics[1]

I.I. Isaeva, M.A. Kharitonov, A.A. Vasilchenko, A.A. Voronin,
A.V. Khoperskov, and E.O. Agafonnikova

Volgograd State University, Volgograd, Russia

✉ isaeva-inessa@mail.ru, ✉ kharitonov@volsu.ru,
✉ aa-vasilchenko@mail.ru, ✉ voronin.prof@gmail.com,
✉ khoperskov@volsu.ru, ✉ agafonnikova@volsu.ru

Abstract. This two-part study presents an approach to designing a sustainable management system for the environmental socio-economic systems (ESESs) of floodplain territories based on modeling their structure dynamics and hydrotechnical projects on their hydrological regime stabilization. The objective of management is to achieve and maintain the optimal stationary complex structure of a floodplain territory, which is characterized by the best design-achievable correspondence between the functional purpose of its fragments and the nature of their spring flooding. The approach rests on the complex structure dynamics model of a floodplain territory that combines variable hydrological and permanent functional properties. This dynamic model, supplemented by an expert model of the socio-economic potentials of the floodplain territory state, yields optimal parameters of hydrotechnical and socio-economic projects. Implementing the approach for a particular floodplain ESES involves optimization, expert assessment, geoinformation and numerical hydrodynamic modeling, high-performance computing, and the statistical analysis of natural observation data and the results of computational experiments. The retrospective, modern, and forecasted complex structures of the northern part of the Volga–Akhtuba floodplain are numerically built considering the spatial heterogeneity of the riverbed degradation effect of the Volga. These numerical results are used to develop an algorithm for finding the parameters of hydrotechnical projects to ensure an optimal sustainable complex structure of the floodplain territory. The algorithm and the results of its numerical implementation will be presented in part II of the study.

Keywords: sustainable development, territorial structure control, hydrotechnical projects, high-performance computing, hydrodynamic modeling, Volga–Akhtuba floodplain.

INTRODUCTION

Floodplain environmental socio-economic systems (ESESs) are characterized by an increased dependence of their condition on the hydrological regime. The complex structure of the channel system and flood inundation zones determines the mosaic arrangement of the functional zones of floodplain territories. The efficient management of floodplain ESESs is based on an optimality measure of correspondence between the territorial distribution of water resources and the functional distribution of floodplain fragments.

The territorial distribution of water resources in floodplain ESESs is formed mainly by the dynamics of their flood inundation (the volume of spring floods, channel structure, and the topography of the territory). The construction of a hydroelectric power stations sys-

---

tem on large rivers, in addition to hydroelectric power generation systems, creates an opportunity to regulate spring floods, which are transformed into the spring discharges of hydroelectric power stations (HPSs). This regulation provides favorable conditions for the operation of floodplain ESESs. However, the gradual erosion (depression) of the riverbed in significant (more than a hundred kilometers) channel zones in the downstream of HPSs due to the violation of the dynamic equilibrium between washout and deposition of bottom soil particles is the reason for the slow lowering of river levels. For example, the decreases in river levels over the years of HPS operation are as follows: for the Kama at the Votkinsk HPS, –1.1 m; for the Volga at the Nizhny Novgorod HPS, –1.3 m; for the Volga at the Volzhsk HPS, from –1.7 m to –1.8 m (low-water conditions) and from –1.25 m to –1.35 m (spring floods) [1–7]. This is the reason for the decreasing volume of flood waters entering the floodplains [1–8].

This decrease results in a progressive narrowing of the stable flooded area, which is the biotope of its environmental system, and the expansion of the unstable flooded area, least valuable for ESESs. Thus, unlike the floodplains of unregulated rivers suffering from floods, those of regulated ones suffer from anthropogenic aridization. Therefore, an urgent problem of their water resources management is to ensure the stability of ecosystems and sustainable socio-economic development under water scarcity.

In past decades, the problem of achieving a rational balance between socio-economic and environmental needs in river systems has been the subject of intensive research [7–26]. The rich list of recent-year publications can be divided into studies on monitoring, detection, and modeling of environmental and socio-economic problems and risks (e.g., see [7–18]) and studies on the design of decision systems [19–25] and risk management [26–29]. Note that the first group of studies involves relatively accurate quantitative (geoinformation, hydrodynamic, and statistical) methods and technologies, whereas the second group is mainly based on qualitative methods of management and expert assessment. Here, the objective reason is the multidimensional uncertainty in the sustainable management of floodplain ESESs.

The sustainable development of river systems and the closely related problem of ecological and economic management of regional ESESs are also the subject of many studies [30–35]. The authors [30–33] focused on the problem of reducing the quality of life and economic efficiency under the anthropogenic degradation of floodplain landscapes and ecosystems. The research topics were methods and technologies for identifying the parameters of sustainable development as well as ensuring their achievement and maintenance. In [33], the problem of sustainable development was analyzed using system compatibility indices; they are calculated based on the objective functions of actors and sustainability criteria for ecosystems. The resulting domain of admissible parameter values is equivalent to the domain of normative lossless actions for the economic agents of the corresponding ESES within its ecological and economic management system [34]. Note that, being adequate for stable systems, these approaches lose their efficiency when analyzing the floodplain ESESs of regulated rivers under developing natural and technogenic degradation. The identification and control of such parameters are significantly complicated due to the absence of long-term deterministic conditioning of flood inundation maps of the territory by the river hydrograph (the time dependence of water discharge through the river channel cross-section). Therefore, the main ground for the sustainable development of floodplains is the long-term stabilization of their hydrological regime.

This paper develops an approach to creating a sustainable management system for floodplain ESESs through optimizing hydrotechnical and socio-economic projects. The objective of management is to achieve and maintain the optimal stationary complex (C) structure of the floodplain territory, which determines the efficiency of the ESES. Optimality is characterized by the best design-achievable correspondence between the functional purpose of floodplain fragments and the nature of their spring flooding. The management problem is solved using geoinformation and numerical hydrodynamic modeling, dynamic programming, high-performance computing, heuristic optimization and expert assessment, and statistical analysis of natural observation data and the results of computational experiments.

The approach is implemented for the northern part of the Volga–Akhtuba floodplain (VAF) located within the Volgograd Region, occupying an area of 867 km^2 with a total length of large and small channels of about 800 km. The Volgo–Akhtuba floodplain has high natural diversity as well as favorable conditions for agriculture, limited housing construction, and ecological tourism. The creation of the Volga hydroelec-

tric power stations system (especially, the Volzhsk HPS in 1961) was the main factor in the formation, operation, and subsequent degradation of the VAF [9, 10]. During spring flooding, over 70% of the VAF territory is flooded from the Akhtuba, a branch of the Volga. During the operation period of the Volzhsk HPS, the average share of water entering the Akhtuba from the Volga during spring flooding has decreased three times [35, 36]. A peculiarity of the Volzhsk HPS is that a significant part of the territory (37%) has the indeterminate cadastral type of land use.

Some elements of the approach and their implementation results were presented in the previous publications. For example, the paper [37] described the concept of the *C*-structure of a floodplain territory as a tool for analyzing its territorial potential. The strategic management problem of a floodplain territory was formulated as follows: achieve the C-structure maximizing the value of the aggregated territorial environmental socio-economic (ESE) potential. The ESE potential of a certain kind was defined as the weighted sum of the products of the area of territorial fragments attributed to that kind by the value of a function characterizing the measure of correspondence between the functional purpose of those fragments and the nature of their spring flooding. The problem was numerically investigated for the modern relief of the VAF territory controlled by a system of dams with variable cross-sections in large and small floodplain channels, and the corresponding simulation results were provided.

The paper [38] described a model of long-term natural and technogenic dynamics for the *C*-structure of the floodplain territory. This model is based on a simplified spatially homogeneous regression model of the technogenic depression of the floodplain channel. Also, the dynamics of the aggregated 12-element C-structure and three ESE potentials of the VAF territory were forecasted up to 2050.

In this paper, we present a long-term dynamics modeling method for the C-structure of the floodplain territories of regulated rivers that includes the following elements: an algorithm for building a set of flood modeling maps (FMMs), a regression model of the spatially heterogeneous depression of the main floodplain channel, an approximate algorithm for building retrospective and forecasted flood inundation maps, a 24-element model of the *C*-structure of the floodplain territory, and an algorithm for building retrospective and forecasted *C*-structures. This method is numerically implemented for the northern part of the Volga–Akhtuba floodplain and the corresponding results are presented. These numerical results are used to develop an algorithm for finding the parameters of hydrotechnical projects to ensure an optimal sustainable complex structure of the floodplain territory. The algorithm and the results of its numerical implementation will be presented in part II of the study.

1. THE METHODS AND TECHNOLOGIES OF THIS STUDY

1.1. Water Dynamics Modeling Tools

Calculations of water dynamics in river channels and the interfluve of the Volga and Akhtuba are based on shallow water equations that consider hydraulic resistance in the Manning model [39, 40]. The EcoGIS-Simulation software package is used for the numerical modeling of surface water movement [41, 42], with a digital elevation model (DEM) of the northern part of the Volga–Akhtuba floodplain [43, 44] as one module. The computational core of EcoGIS-Simulation involves CSPH-TVD, a numerical two-step algorithm for integrating hydrodynamic equations that combines the Lagrange and Euler approaches (Smoothed-ParticleHydrodynamics and TotalVariationDiminishing, respectively) [45, 46]. Parallel computations are performed on NVIDIA Tesla GPUs [39, 47].

1.2. The Set of Flood Modeling Maps

The calculations of water dynamics during the spring discharge of the HPS in year τ (see subsection 1.1) yield a series of flood inundation maps $\mathrm{K}_\tau^{\mathrm{in}}(t_k) = \mathrm{K}^{\mathrm{in}}(Q_\tau(t), t_k)$, $t \in [t_0, t_k]$, $k = 1, ..., k_{\max}$, where t_0 denotes the time instant of discharge start and $Q_\tau(t)$ is the hydrograph of the spring discharge of the HPS in year τ (Q_τ is the flow rate, and t indicates time, h). The digital flood inundation map of a territory is a two-dimensional array, where each element (i, j), $i = 1, ..., N$, $j = 1, ..., M$, at each time instant t_k shows the water height $h_{ij}(t_k)$ and its velocity vector $v_{ij}(t_k)$. Due to the geoinformation and hydrodynamic modeling error ε_g, it is required to calculate the minimum flood height $h_{\min}$: under the inequality $h_{ij}(t_k) \geq h_{\min}$, the corresponding cell of the digital map

is "flooded" at the time instant t_k. (The origin, algorithm, and results of calculating the values ε_g and h_{min} were described in [48].) With each map $\mathrm{K}^{in}(Q(t), t_k)$ we associate the map $\mathrm{K}(Q(t), t_k)$, where each cell contains the variable $m_{ij} = \{0, 1\}$, $i = 1, ..., N$, $j = 1, ..., M : m_{ij} = 0$ if $h_{ij}(t_k) < h_{min}$, and $m_{ij} = 1$ if $h_{ij}(t_k) \geq h_{min}$. In each of the numerous computational experiments with the real and model hydrographs $Q(t)$, there was a time instant t^{max} with the largest number of flooded cells in the map $\mathrm{K}(Q(t), t^{max})$. Such maps are used in this paper.

When varying $Q(t)$ and the control vector u that changes the relief of the flooded territory or the safe flooding conditions, the computational complexity of building a large number of digital maps $\mathrm{K}^{in}(Q(t), t^{max}, u)$ and the corresponding maps $\mathrm{K}(Q(t), t^{max}, u)$ can be reduced by replacing, with an error $\varepsilon_c \leq \varepsilon_g$, each multistage hydrograph $Q(t)$ with a constant hydrograph $G^c = (Q^c, t^{max})$, characterized by the constant flow Q^c and the duration t^{max}. Note that $\varepsilon_c = \max(\varepsilon_1, ..., \varepsilon_L)$, where the errors $\varepsilon_l (l = 1, ..., L)$ characterizing the relative differences between the maps $\mathrm{K}_l^{(1)}(Q(t))$ and $\mathrm{K}_l^{(2)}(Q^c, t)$ are given by

$$\varepsilon_l = \left(\min\left(\sum_{j=1}^{M}\sum_{i=1}^{N} m_{ijl}^{(1)}, \sum_{j=1}^{M}\sum_{i=1}^{N} m_{ijl}^{(2)} \right) \right)^{-1} \sum_{j=1}^{M}\sum_{i=1}^{N} \left| m_{ijl}^{(1)} - m_{ijl}^{(2)} \right|,$$

where $m_{ijl}^{(p)} = 0$ if the cell (i, j), $i = 1, ..., N$, $j = 1, ..., M$, of the digital map $\mathrm{K}_l^{(p)}(p = 1, 2)$ is not flooded, and $m_{ijl}^{(p)} = 1$ otherwise. The hydrographs are replaced by a heuristic algorithm: on each time interval $[t_0, \tilde{t}]$, the step hydrograph $Q(t)$ is replaced by a constant hydrograph of equal volume with the corresponding flow rate Q_i^c. The value $t^{(1)} = \arg\max_{\tilde{t}}[Q_{\tilde{t}}^c]$ preliminarily estimates the maximum flood time instant. This value is refined by calculating the relative difference function $\varepsilon(\eta)$ between the maps $\mathrm{K}^{(1)}(Q(t))$ and $\mathrm{K}_\eta^{(2)}(Q_{t_\eta^{max}}^c, t_\eta^{max})$, where

$t_\eta^{max} = t^{(1)}\left(1 + \eta(t_1 - t_0) \times (t^{(1)} - t_0)^{-1}\right)$, and t_1 is the root of the equation $Q_{t^{(1)}}^c = Q(t_1)$. The most accurate estimate is t_*^{max}, where $\eta^* = \arg\min_\eta \varepsilon(\eta)$. Let us denote $t_{\eta^*}^{max} \equiv t^{max}$.

The maps $\mathrm{K}(Q^c, t^{max})$ are built using the set of FMMs, which contains an array of floodplain inundation maps with constant hydrographs $G_{ij}^c = (Q_i^c, t_j)$ and the modern topography of channel bottom and flooded territory. This set is formed so that the relative differences between the maps $\mathrm{K}(G_{ij}^c)$ and $\mathrm{K}(G_{i+1,j}^c)$ as well as between the maps $\mathrm{K}(G_{ij}^c)$ and $\mathrm{K}(G_{i,j+1}^c)$ do not exceed ε_g. The map $\mathrm{K}(G_{ij}^c)$ $(Q_i^c \leq Q^c \leq Q_{i+1}^c, t_j \leq t^{max} \leq t_{j+1})$ is selected as the map $\mathrm{K}(Q^c, t^{max})$ for calculating target flooding and environmental safety conditions. The map $\mathrm{K}(G_{i+1,j+1}^c)$ is selected as the map $\mathrm{K}(Q^c, t^{max})$ for calculating socio-economic safety conditions.

1.3. The Regression Model of Main Channel Depression and the Approximate Algorithm for Building Floodplain Inundation Maps

The progressive natural-technogenic depression of the main channel is modeled by the regression dependence $h(Q^c, \tau, L)$, $(\tau \in [\tau_0, \tau_0 + N]$, in years) of the water level h on the hydrograph Q^c at the distance L from the downstream of the HPS according to the long-term measurements of water levels $h_i(Q(t_j), \tau, L_i)$, $i = 1, ..., I$, $j = 1, ..., J$, $\tau \in [\tau_0, \tau_0 + N]$, at I gauging stations located at the distances L_i from the downstream of the HPS. The regression equation describing the spatial heterogeneity of the channel depression effect has the form

$$h(w) = (a, w) + w^{\mathrm{T}} A w + b, \quad w = (Q^c, \tau, L)^{\mathrm{T}},$$
$$a = (a_1, a_2, a_3), \quad A = \|a_{ij}\|_{i,j=1}^{3}. \tag{1}$$

The expression (1) allows finding a virtual hydrograph $Q_2^c = \varphi(Q_1^c, \tau_1, \tau_2, L)$, a function of the variable L, which is a solution of the equation $h(Q_1^c, \tau_1, L)$

$= h(Q_2^c, \tau_2, L)$. For any $t^{\max}$, the virtual hydrograph $(\varphi(Q_1^c, \tau_1, \tau_2, L), t^{\max})$ provides flooding of the territory under the channel state in year τ_2 that is equivalent to flooding of the territory with the constant hydrograph $(Q_1^c, t^{\max})$ under the channel state in year τ_1.

The L-variable hydrograph is approximated by an L-stepped hydrograph to build a rather accurate retrospective or forecasted flood inundation map of the territory in year τ_2 as the composition (gluing) of separate fragments from the set of flood modeling maps (based on the relief in year $\tau_1 = 2022$) with different values of the constant flow Q_j^c and the modeling error $\varepsilon_c = \max(\overline{A}, \varepsilon_g)$, where $\overline{A}$ denotes the average approximation error of (1). The map fragments approximating those of the flood inundation map $\tilde{K}_k(\varphi(Q_1^c, \tau_1, \tau_2, L), t^{\max})$: $\tilde{K}(\varphi(Q_1^c, \tau_1, \tau_2, L), t^{\max})$, $L_k \leq L \leq L_k + \Delta L$, $k = 1,..., K-1$, $L_1 = 0$, are the corresponding fragments $K_k(G_{ij}^c)$ of the maps from the set of FMMs: $Q_i^c \leq \varphi(Q_1^c, \tau_1, \tau_2, L) \leq Q_{i+1}^c$, $t_j \leq t^{\max} \leq t_{j+1}$, $L_k \leq L \leq L_k + \Delta L$. Here, $L_{\max}$ is the length of the modeled part of the channel; ΔL_k, $k = 1,..., K-1$, are the roots of the equations $\varphi(Q_1^c, \tau_1, \tau_2, L_k + \Delta L_k) - \varphi(Q_1^c, \tau_1, \tau_2, L_k) = Q_{i+1}^c - Q_{i+1}^c$, providing the required accuracy; the values K and ΔL are determined by the relations $\sum_{k=1}^{K} \Delta L_k = L_{\max} = K \Delta L$.

1.4. The Complex Structure Model of a Floodplain Territory

The elements of the primary functional (F) structure are the sets of local fragments of a territory with the same cadastral type of land use (F-kinds). The elements of aggregated F-structures are their unions into groups (F-types) on various grounds. The F-structure of a floodplain territory is built based on its digital cadastral map.

The elements of the hydrological (H_1) structure are the sets of local fragments of the territory with the same frequency ranges of their flood inundation (H_1-kind). The number of frequency ranges and their boundaries are determined, on the one hand, by the objectives of the study and, on the other hand, by the possibility of their identification with a given accuracy. The enlarged frequency ranges form H_1-types. The complex structure of a floodplain territory is the superposition of its H_1- and F-structures. The elements of the C-structure are the sets of its local fragments with the same H_1-kind (type) and the same F-kind (type). The existence of the structure $H_1(\tau)$ is determined by the stability of the relief, channel structure, and distribution function of the annual flood hydrograph volume calculated for samples. The size Θ of such samples (the number of consecutive years of observations corresponding to the interval $\left[\tau - \dfrac{\Theta}{2}, \tau + \dfrac{\Theta}{2} - 1\right]$) is determined based on the requirements for the identification accuracy. An algorithm for calculating the minimum value Θ was described in [37]. In this study, we use the enlarged frequency ranges (H_1-types) characterizing the following territories: stable flooded (with a frequency equal to or exceeding some threshold $n^{\lim}$), unstable flooded (with a frequency below $n^{\lim}$), and non-flooded (never flooded during the observation period). The ESE potentials of F-structure elements are estimated using characteristic functions reflecting the measure of correspondence between their F-kind (type) and the H_1-kind (type). The characteristic functions are built by experts.

If the H_1- and F-structures contain n and m elements, respectively, they will form the C-structure of nm elements. An algorithm for building a 12-element C-structure based on a three-element H_1-structure and a four-element F-structure (social, environmental, economic, and uncertain territories) was described in detail in [37], including the resulting C-structure as well. However, this F-structure has a disadvantage: it provides no classification for the territorial fragments of floodplains. Therefore, in this paper, we adopt the aggregated functional structure F_1 as a set of eight typical elements, each being described by one of the three typical characteristic functions: social (S, φ_3), environmental (En, φ_1), economic (Ec, φ_3), environmental-economic (EnEc, φ_1), social-environmental (SEn, φ_1), socio-economic (SEc, φ_3), environmental socio-economic (EnSEc, φ_1), and indeterminate (I, φ_2). The

latter type means no cadastral land use. The characteristic functions φ_1, φ_2, and φ_3 have the following form:

$$\varphi_1(n) = \begin{cases} 0, & 0 \leq n < n^{\lim}, \\ 1, & n^{\lim} \leq n \leq 1; \end{cases}$$

$$\varphi_2(n) = 1;$$

$$\varphi_3(n) = \begin{cases} 0, & 0 < n \leq 1, \\ 1, & n = 0. \end{cases}$$

The superposition of the F_1-structure and the three-element H_1-structure forms the 24-element C-structure $K_{24}(\tau)$, used below to solve the management problem.

1.5. The Dynamics Model of the H_1-structure

As mentioned above, the channel depression effect leads to changes in the H_1-structure over time. The dynamics model of this structure is a set of algorithms for building a sequence $H_1(\tau)$, $\tau = \tau_0, ..., \tau_0 + N, ..., T$. This sequence consists of real ($H_1^r(\tau)$) and model ($H_1^{\mod}(\tau)$) structures. The real structures $H_1^r(\tau)$, corresponding to the case $\tau_0 + \dfrac{\Theta}{2} \leq \tau \leq \tau_0 + N - \dfrac{\Theta}{2} + 1$, are built using a set of flood inundation maps for the observation period with the hydrographs G_θ^c, $\theta \in \left[\tau - \dfrac{\Theta}{2}, \tau + \dfrac{\Theta}{2} - 1 \right]$, obtained by the algorithm from subsection 1.3. (On the stable flood inundation map $K_\tau^{n^{\lim}}$ of the structure $H_1^r(\tau)$, a flooded cell is the one flooded on at least $n^{\lim}\Theta$ maps of the set containing Θ maps.)

The model structures $H_1^{\mod}(\tau)$ are formed for the cases where the sampling interval, fully or partially, exceeds the boundaries of the observation period ($\tau < \tau_0 + \dfrac{\Theta}{2}$ or $\tau > \tau_0 + N - \dfrac{\Theta}{2} + 1$). In the paper [37], these structures were built using flood inundation maps calculated considering the spatially homogeneous depression effect of the main channel in year τ with the virtual model hydrographs G_i^c, $i = 1, ..., \Theta$, whose parameters were randomly selected from the general population.

If the algorithm [37] is applied to build a large number of the model structures $H_1^{\mod}(\tau)$ corresponding to different hydrotechnical projects considering the spatially heterogeneous depression effect of the main channel, the computational complexity of the algorithm for solving the management problem will increase significantly. Therefore, in this study, a less computationally intensive algorithm is used to build approximate model structures. This algorithm is to find the generalized hydrograph $\widehat{G}_o^c = (\widehat{Q}_o^c, \widehat{t}_o)$ and the nearest hydrograph from the set of FMMs $G_{ij}^c = (Q_i^c, t_j)$, $Q_i \leq \widehat{Q}_o^c \leq Q_{i+1}$, $t_j \leq \widehat{t}_o \leq t_{j+1}$, whose map best approximates the set of stable flood inundation maps $K_\tau^{n^{\lim}}$ in the virtual structures $H_1^v(\tau)$ generated for the entire observation period $\tau_0 + \dfrac{\Theta}{2} \leq \tau \leq \tau_0 + N - \dfrac{\Theta}{2} + 1$ using the flood inundation maps based on the modern relief of the main channel with the hydrographs G_θ^c, $\theta \in \left[\tau - \dfrac{\Theta}{2}, \tau + \dfrac{\Theta}{2} - 1 \right]$. (These structures would coincide with the real ones in the absence of channel depression.)

The hydrograph $\widehat{G}^c = (\widehat{Q}^c, \widehat{t})$ is found as follows. For the parameters Q_τ^c and $t_\tau^{\max}$ of the set of hydrographs G_τ^c ($\tau = \tau_0, ..., \tau_0 + N$), the linear regression $Q^c = a t^{\max} + b$ is constructed. For each fixed $\tau = \tau_0 + \dfrac{\Theta}{2}, ..., \tau_0 + N - \dfrac{\Theta}{2} + 1$ and each hydrograph G_θ^c, $\theta \in \left[\tau - \dfrac{\Theta}{2}, \tau + \dfrac{\Theta}{2} - 1 \right]$, the virtual hydrograph $\tilde{G}_\theta^c(\tau)$ of the volume $V_\theta = Q_\theta^c t_\theta^{\max}$ is calculated so that the parameters $\tilde{Q}_\theta^c$ and $\tilde{t}_\theta^{\max}$ lie on this regression. These hydrographs are ordered by volume. The approximate steady-state flood inundation map $\tilde{K}_\tau^{n^{\lim}}$ is the one of the hydrograph $\tilde{G}_\tau = (\tilde{Q}_\tau^c, \tilde{t}_\tau^{\max})$ with the serial number $\left[n^{\lim}\Theta \right] + 1$. The error ε_τ of determining the map $\tilde{K}_\tau^{n^{\lim}}$ is the relative share of cells whose flooding character differs in the maps $\tilde{K}_\tau^{n^{\lim}}$ and $K_\tau^{n^{\lim}}$ (see the algorithm in subsection 1.2). If the average value of these errors does not exceed ε_m, then the weighted average values of the parameters $\widehat{Q}_o^c$ and $\widehat{t}_o$

of the generalized hydrograph $\hat{G}_o^c$ are determined using the linear regression and the equation $\hat{Q}^c \hat{t} = (N - \Theta)^{-1} \sum_\tau \tilde{Q}_\tau^c \tilde{t}_\tau^{\max}$. The hydrograph closest to $\hat{G}_o^c$ from the set of FMMs $G^{\mathrm{st}} = (Q^{\mathrm{st}}, t^{\mathrm{st}}) = (Q_i^c, t_j)$, $Q_i \le \hat{Q}_o^c \le Q_{i+1}, t_j \le \hat{t}_o \le t_{j+1}$, is the desired result. This approximation has the error $\varepsilon_s = (N - \Theta)^{-1} \sum_\tau \varepsilon_\tau$. To build the retrospective and forecasted structures $H_1^{\mathrm{mod}}(\tau)$ using the set of FMMs, it is necessary to calculate the variable hydrograph $G_\tau^{\mathrm{st}}(L) = (\varphi(Q^{\mathrm{st}}, 2022, \tau, L), t^{\mathrm{st}})$ and form flood inundation maps from the fragments of maps of this set (see the algorithm in subsection 1.3). The resulting approximate structures $H_1^v(\tau)$, $H_1^r(\tau)$, and $H_1^{\mathrm{mod}}(\tau)$ are used to build the corresponding approximate 24-element complex structures $K_{24}^v(\tau)$, $K_{24}^r(\tau)$, and $K_{24}^{\mathrm{mod}}(\tau)$. The hydrological structures built from the flood inundation maps calculated for floodplain channel bed reliefs with projected dams are called the projected structures $K_{24}^{pr}(\tau)$.

In addition to the structure H_1, the algorithm for optimizing hydrotechnical projects involves the hierarchical hydrological structure H_2 of the floodplain territory (a set of its fragments, i.e., zones flooded from channel systems formed by branches from the principal main channel. This algorithm will be presented in part II of the study. One part of the zones is formed by dead-end branches; the other part, by medium main channels (MMC). The territorial fragments flooded from separate channels form microzones. The error of determining the zone boundary, equal to the volume of transboundary water flows divided by the volume of water entering the zone from its channels, may exceed ε_g. In this case, the zone joins the neighbor one, forming a macro-zone. The algorithm and the numerical results of building the structure H_2 of the VAF were described in [49].

2. THE RETROSPECTIVE, MODERN, AND FORECASTED *C*-STRUCTURES OF THE NORTHERN PART OF THE VOLGA–AKHTUBA FLOODPLAIN

According to the results of computational experiments, the error of open-data satellite measurements for VAF relief elevations (with an absolute value of 0.5 m) causes the hydrodynamic modeling error of digital flood inundation maps. The relative value of the latter error is calculated by the algorithm from subsection 1.2 and does not exceed $\varepsilon_g = 0.05$ [48]. To implement the algorithms described above, the set of FMMs with the hydrographs of the Volzhsk HPS $G_{ij}^c = (Q_i^c, t_j)$, $13\,000 \le Q_i^c \le 28\,000$ m³/s, $0 \le t_j \le 960$ h, was created. This set contains over 3500 maps built with a relative error not exceeding $\varepsilon_g = 0.05$.

The coefficients of the regression (1) for the Volga levels downstream of the Volzhsk HPS were calculated based on the official hydrological data on water level dynamics at four gauging stations: the downstream of the Volzhsk HPS, Volgograd (the river port), Svetly Yar, and Cherny Yar (see the website of PJSC RusHydro). Figure 1 shows the water level dynamics at these gauging stations under low-water flow values. Also, the linear trends of water level changes for $Q^c = 4\,000, 5\,000, 6\,000$ m³/s and the average annual water level decreases $\delta\eta$ are presented. For the downstream of the Volzhsk HPS, $\delta\eta = -0.0201$ m; for Svetly Yar (65 km from the Volzhsk HPS), $\delta\eta = -0.0108$ m. In the vicinity of Cherny Yar, the bottom depression almost disappears. These estimates give a total depression of about 1.25 m for the downstream of the Volzhsk HPS on the time horizon 1961–2023.

The statistically significant coefficients of the regression (1) describing the depression of the Volga channel downstream of the Volzhsk HPS are $a_1 = 3.00 \cdot 10^{-4}$, $a_2 = -2.25 \cdot 10^{-2}$, $a_3 = -5.35 \cdot 10^{-4}$, $a_{23} = a_{32} = 1.17 \cdot 10^{-7}$, and $b = 32.54$. The average approximation error is $\bar{A} = 0.097$.

Thus, the depression of the Volga channel downstream of the Volzhsk HPS is described by the regression (1) of the form

$$h(Q^c, \tau, L) = a_1 Q^c + a_2 \tau + a_3 L + 2a_{23}\tau L + b. \quad (2)$$

The function $\varphi(Q_1^c, \tau_1, \tau_2, L)$ (see subsection 1.3) built using the regression (2) has the form

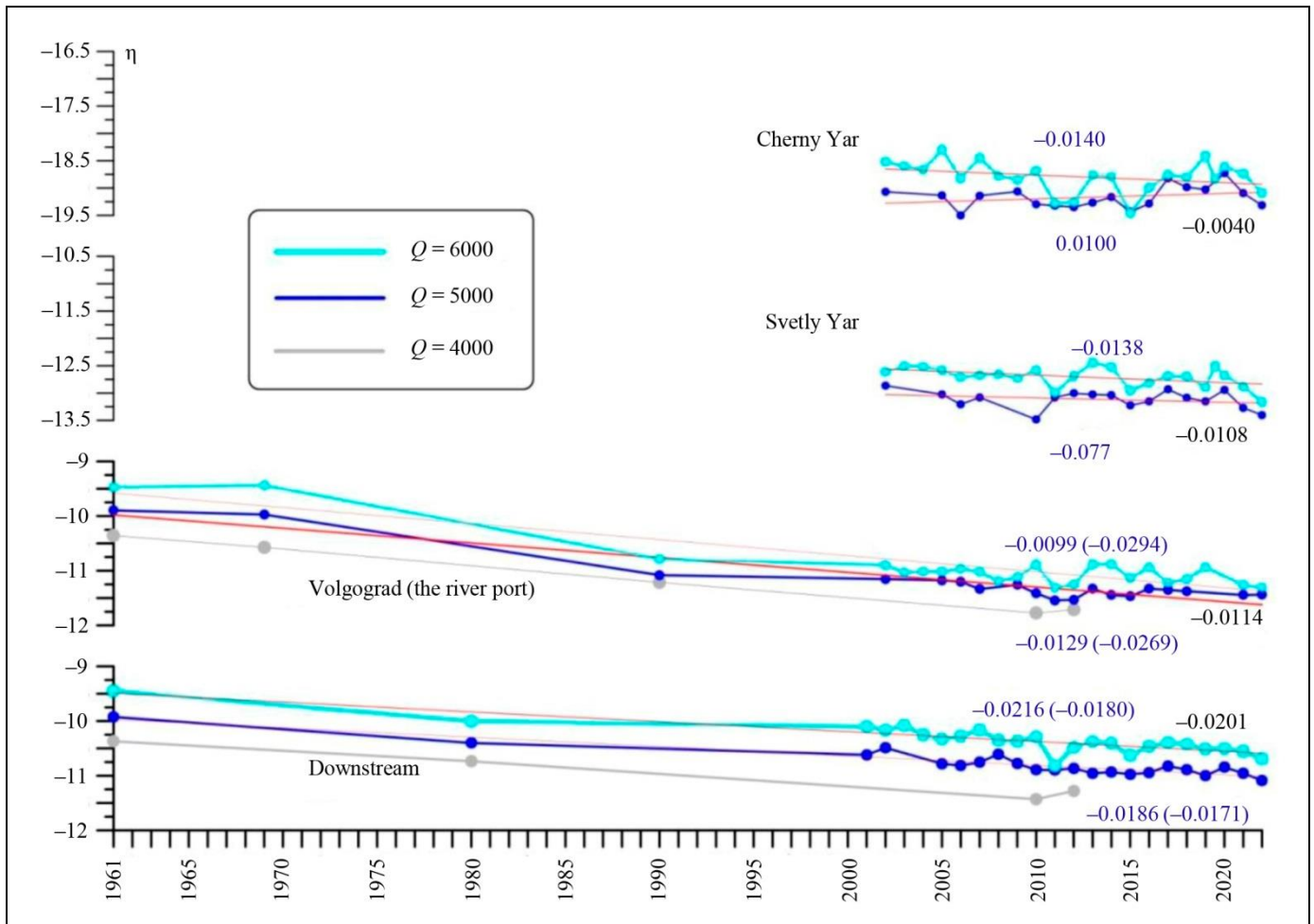$$\varphi(Q_1^c, \tau_1, \tau_2, L) = Q_1^c - \frac{(a_2 + 2a_{23}L)}{a_1}(\tau_2 - \tau_1). \quad (3)$$

Fig. 1. Measurements at four gauging stations downstream of the Volzhsk HPS dam. The blue color indicates the average annual water level decrease at a gauging station considering all data. Similar values for the period since 2001 are given in brackets. The black color indicates the values averaged over Q.

In view of (3), the virtual discharges—the basis of the algorithms for building the retrospective $K_{24}^r(1975)$, modern $K_{24}^r(2005)$, and forecasted $K_{24}^{\mathrm{mod}}(2052)$ *C*-structures (see subsections 1.3–1.5)—are calculated by the formulas

$$Q_{1975}^c(Q_{2022}^c, L) = Q_{2022}^c - 3525 - 0.0367L,$$

$$Q_{2005}^c(Q_{2022}^c, L) = Q_{2022}^c - 1275 - 0.0133L, \qquad (4)$$

$$Q_{2052}^c(Q_{2022}^c, L) = Q_{2022}^c + 2250 - 0.0235L.$$

When gluing the flood inundation maps from the set of FMMs to ensure the required accuracy $\varepsilon_c = \max(0.05; 0.097) = 0.097$ (see the algorithm in subsection 1.3), each map within the territory was built from nine fragments of the maps from the set of FMMs, whose parameters were found by formulas (4). The length of each map fragment along the Volga

channel was $\Delta L = 7500\,\mathrm{m}$. The difference in the Volga discharge values for neighbor map fragments was $\Delta Q = 250\,\mathrm{m}^3/\mathrm{s}$.

When building all *C*-structures, the sample size $\Theta = 30$ and $n^{\lim} = 0.85$ were selected. The regression equation $Q = 237t + 23117$ was used to find the hydrograph $\hat{G}^c = (\hat{Q}^c, \hat{t}_c)$ in accordance with the algorithm from subsection 1.5. In turn, this hydrograph served to build the approximate projected structures $H_1^{\mathrm{mod}}(2052)$ of the Volzhsk HPS. The resulting parameters $\tilde{Q}_\tau^c$ and $\tilde{t}_\tau^{\max}$ of the approximate hydrographs $\tilde{G}_\tau$ of the Volzhsk HPS, used to build the generalized hydrograph $\hat{G}_o^c$ and the nearest hydrograph from the set of FMMs G^c, as well as the relative approximation errors ε_τ, $\tau = 1975, \ldots, 2005$, are presented in the table

below. The hydrograph parameters calculated from these data are $\widehat{G}_o^c = (24\,302,5)$ and $G^{st} = (24\,250,5)$. The stable decrease in the value ε_τ as τ increases can be explained by the transition of the Volzhsk HPS in recent decades to a relatively constant planned two-stage hydrograph of spring discharges.

The value $Q^{st} = 24\,250$ m^3/s was used in formulas (4) to find map fragments from the set of FMMs when building maps and calculating the areas of the elements of the retrospective $K_{24}^r(1975)$, modern $K_{24}^r(2005)$, and forecasted $K_{24}^{mod}(2052)$ C-structures of the VAF (see Figs. 2 and 3). In Fig. 3, the 12 zones of the structure H_2 are also marked by solid lines. Colors indicate stable flooded (green and yellow), unstable flooded (blue and orange), and non-flooded (purple and red) structural elements. Figure 4 shows the maps of the stable flooded territory corresponding to these structures. According to the analysis of these figures, the VAF territory is mainly occupied by the land of the environmental, social-environmental, environmental-economic, and indeterminate cadastral types. Direct comparison of the structures $K_{24}^r(1975)$, $K_{24}^r(2005)$, and $K_{24}^{mod}(2052)$ in Figs. 2–4 demonstrates the progressive natural-technogenic degradation of the VAF stable flooded territory (a biotope of its floodplain ecosystem) and C-structure (a determinant for the efficiency of its socio-economic system). For example, the forecasted decrease in the stable flooded area for 77 years is 62%, including 44% for environmental, 78% for environmental-economic, and 60% for indeterminate types.

The parameters of approximate hydrographs of the Volzhsk HPS for building the generalized hydrograph and approximation errors

τ	$\tilde{Q}_\tau^c$	$\tilde{t}_\tau^{max}$	ε_τ
1975	24539	6	0.0837
1976	24539	6	0.0835
1977	24539	6	0.0705
1978	24302	5	0.0644
1979	24302	5	0.0641
1980	24302	5	0.0640
1981	24302	5	0.0640
1982	24302	5	0.0637
1983	24302	5	0.0554
1984	24302	5	0.0552
1985	24539	6	0.0552
1986	24302	5	0.0548
1987	24302	5	0.0528
1988	24302	5	0.0522
1989	24539	6	0.0511
1990	24539	6	0.0508
1991	24302	5	0.0458
1992	24302	5	0.0457
1993	24302	5	0.0457
1994	24302	5	0.0455
1995	24302	5	0.0408
1996	24302	5	0.0408
1997	24302	5	0.0405
1998	24302	5	0.0377
1999	24302	5	0.0375
2000	24302	5	0.0375
2001	24302	5	0.0371
2002	24302	5	0.0327
2003	24302	5	0.0325
2004	24302	5	0.0316
2005	24302	5	0.0307
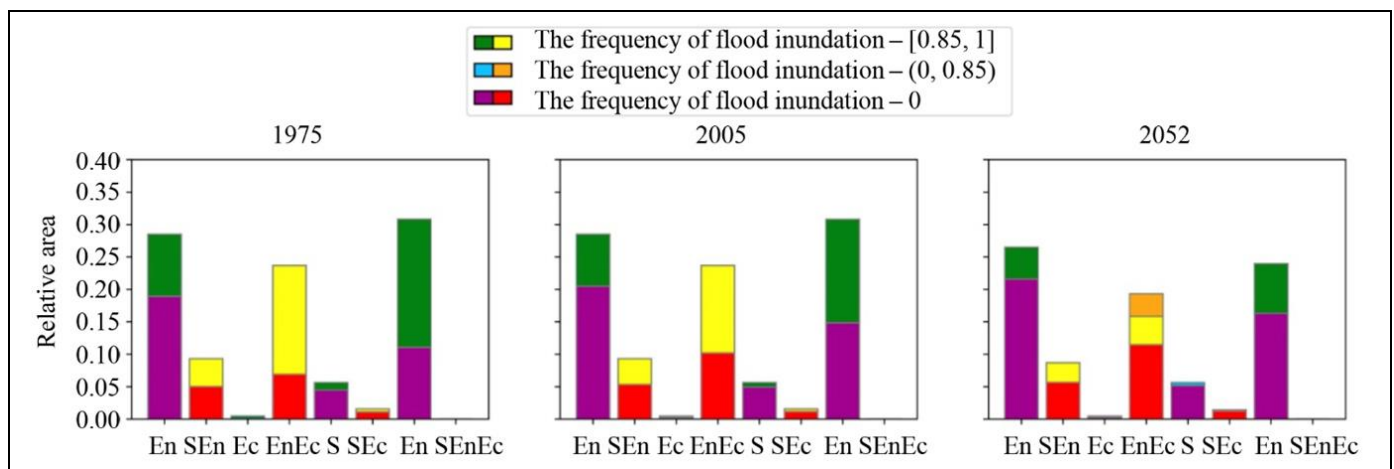
Fig. 2. The diagrams of areas of environmental (En), social-environmental (SEn), economic (Ec), environmental-economic (EnEc), indeterminate (I), and social-environmental (SEn) elements of the C-structures $K_{24}^r(1975)$, $K_{24}^r(2005)$, and $K_{24}^{mod}(2052)$ of the VAF territory.
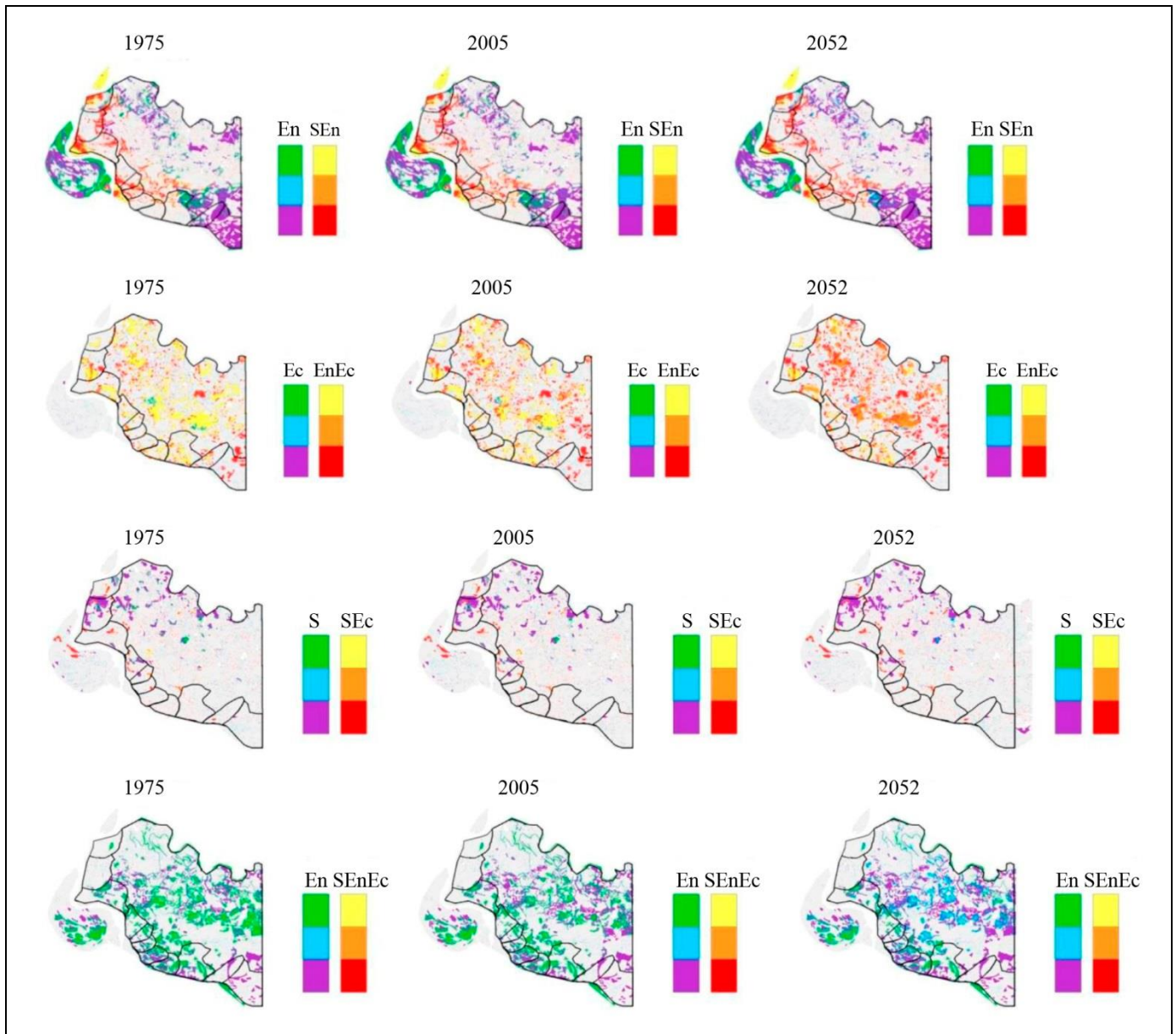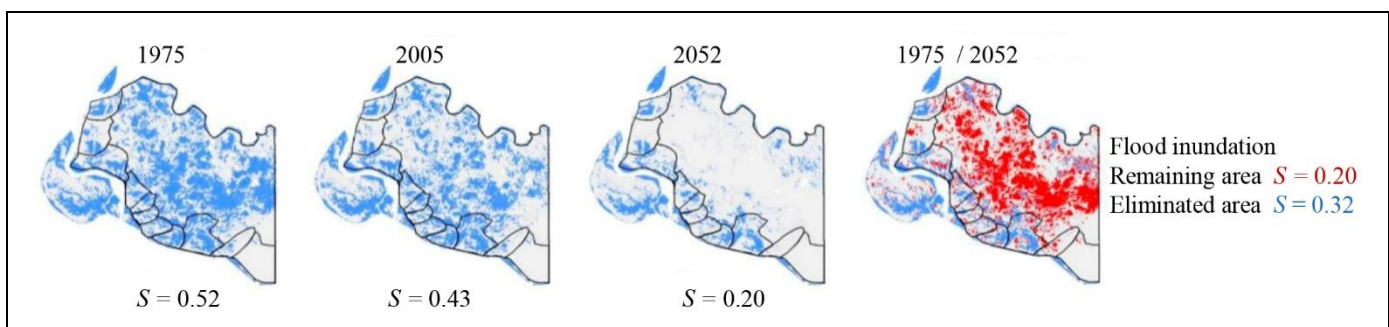
Fig. 3. The maps of environmental (En), social-environmental (SEn), economic (Ec), environmental-economic (EnEc), indeterminate (I), and social-environmental (SEn) elements of the *C*-structures $K_{24}^r(1975)$, $K_{24}^r(2005)$, and $K_{24}^{mod}(2052)$ of the VAF territory.

Fig. 4. The maps and relative areas of stable flooded territory in the *C*-structures of the VAF: retrospective $K_{24}^r(1975)$, modern $K_{24}^r(2005)$, and forecasted $K_{24}^{mod}(2052)$.

CONCLUSIONS

This paper has presented a long-term dynamics modeling method for the C-structure of the floodplain areas of regulated rivers that includes the following elements: an algorithm for building a set of flood modeling maps (FMMs), a regression model of the spatially heterogeneous depression of the main floodplain channel, an approximate algorithm for building retrospective and forecasted flood inundation maps, a 24-element model of the *C*-structure of the floodplain territory, and an algorithm for building retrospective and forecasted C-structures. Implementing this method for a particular floodplain territory involves optimization, expert assessment, geoinformation and numerical hydrodynamic modeling, high-performance computing, and the statistical analysis of natural observation data and the results of computational experiments.

The method has been numerically implemented for the northern part of the Volga–Akhtuba floodplain are the corresponding results have been provided. They demonstrate the progressive natural-technogenic degradation of the VAF stable flooded territory (a biotope of its floodplain ecosystem) and C-structure (a determinant for the efficiency of its socio-economic system). According to these results, hydrotechnical projects are needed to stabilize the hydrological structure of the VAF. Due to the territorial distribution and variability of the parameters of hydrotechnical projects, it is topical to find the optimal *C*-structure.

The models and the results of their numerical implementation are used to develop an algorithm for finding the parameters of hydrotechnical projects to ensure an optimal sustainable C-structure of the floodplain territory. This algorithm and the results of its numerical implementation for the northern part of the Volga–Akhtuba floodplain will be presented in part II of the study.

REFERENCES

1. Ivanov, V.V. and Korotaev, V.N., The Influence of Hydropower Plants on Deformations of Floodplain Banks and Channel Forms in the Lower Reaches of the Volga and Kuban Rivers, in *Eroziya pochv i ruslovye protsessy* (Soil Erosion and Channel Processes), 2008, no. 16, pp. 224–242. (In Russian.)

2. Aleksandrovskii, A.Y., Silaev, B.I., Chukanov, V.V., The Effect of Afterbay Bed Strains on the Performance of Power-Generating Equipment of a Hydropower Plant, *Power Technology and Engineering*, 2002, vol. 36, pp. 323–326.

3. Asarin, A.E. and Tkachev, K.V., Channel Deformations in the Afterbay of the Volgograd Hydropower Plant and Possibilities of Their Limitation, *Gidrotekhnicheskoe Stroitel'stvo*, 2014, no. 12, pp. 54–58. (In Russian.)

4. Bulanov, E.P., Lowering of the Discharge Curve in the Afterbay of the Volzhsk HPS Due to General Scouring of the Chan-

nel, *Doklady i kratkie soobshcheniya 15-go plenarnogo mezhvuzovskogo koordinatsionnogo soveshchaniya po probleme eroziinykh, ruslovykh i ust'evykh protsessov* (Reports and Short Communications of the 15th Plenary Interuniversity Coordination Meeting on the Problem of Erosion, Channel and Mouth Processes), Volgograd–Moscow: Peremena, 2000. (In Russian.)

5. Mazhbits, G.L. and Bulanov, E.P., Changes in the Position of the Discharge–Water Level Curve and Channel Processes in the Afterbay of the Volzhsk HPS, *Materialy Vserossiiskoi nauchno-prakticheskoi konferentsii "Vodnye resursy Volgi: nastoyashchee i budushchee, problemy upravleniya"* (Proceedings of the All-Russian Scientific and Practical Conference "Volga Water Resources: Present and Future, Management Problems"), Astrakhan, 2007. (In Russian.)

6. Górski, K., van den Bosch, L.V., van de Wolfshaar, K.E., et al., Post-damming Flow Regime Development in a Large Lowland River (Volga, Russian Federation): Implications for Floodplain Inundation and Fisheries, *River Research and Applications*, 2012, vol. 28, no. 8, pp. 1121–1134.

7. Hohensinner, S., Grupe, S., Klasz, G., and Payer, T., Long-Term Deposition of Fine Sediments in Vienna's Danube Floodplain before and after Channelization, *Geomorphology*, 2022, vol. 398, art. ID 108038. DOI: 10.1016/j.geomorph.2021.108038.

8. Veksler, A.B. and Donenberg, V.M., *Pereformirovanie rusla v nizhnikh b'efakh krupnykh elektrostantsii* (Reshaping the Channel in the Development of Large Power Plants), Moscow: Energoatomizdat, 1983. (In Russian.)

9. Jardim, P.F., Melo, M.M.M., Ribeiro, L.D.C., et al., A Modeling Assessment of Large-Scale Hydrologic Alteration in South American Pantanal Due to Upstream Dam Operation, *Frontiers in Environmental Science*, 2020, vol. 8, art. ID 567450. DOI: 10.3389/fenvs.2020.567450.

10. Bolgov, M.V., Shatalova, K.Yu., Gorelits, O.V., et al., Water and Ecology Problems of the Volga–Akhtuba Floodplain, *Ecosystems: Ecology and Dynamics*, 2017, vol. 1, no. 3, pp. 15–37. (In Russian.)

11. Zemlyanov, I.V., Gorelits, O.V., Pavlovskii, A.E., et al., Analysis of Environmental Impacts of the Volgograd Reservoir Operation on Biodiversity Conservation in the Main Wetland Areas of the Lower Volga Basin, *Research Report of Zubov State Oceanographic Institute*, Moscow, 2010. (In Russian.)

12. Fernandes, M.R., Aguiar, F.C., Martins, M.J., et al., Long-Term Human-Generated Alterations of Tagus River: Effects of Hydrological Regulation and Land-Use Changes in Distinct River Zones, *Catena*, 2020, vol. 188, art. ID 104466. DOI: 10.1016/j.catena.2020.104466.

13. Li, W.-J., Yu, S.-Y., Pan, J., et al., A 2000-Year Documentary Record of Levee Breaches on the Lower Yellow River and Their Relationship with Climate Changes and Human Activities, *Holocene*, 2021, vol. 31, no. 3, pp. 333–345.

14. Lu, C., Jia, Y., Jing, L., et al., Shifts in River-Floodplain Relationship Reveal the Impacts of River Regulation: A Case Study of Dongting Lake in China, *Journal of Hydrology*, 2018, vol. 559, pp. 932–941. DOI: http://dx.doi.org/10.1016/j.jhydrol.2018.03.004.

15. Ablat, X., Wang, Q., Arkin, N., et al., Spatiotemporal Variations and Underlying Mechanism of the Floodplain Wetlands in the Meandering Yellow River in Arid and Semi-arid Regions, *Ecological Indicators*, 2022, vol. 136, art. no. 108709. DOI: https://doi.org/10.1016/j.ecolind.2022.108709.

16. Wu, C., Webb, J.A., and Stewardson, M.J., Modelling Impacts of Environmental Water on Vegetation of a Semi-Arid Floodplain–Lakes System Using 30-Year Landsat Data, *Remote Sens.*, 2022, vol.14, no. 3, art. no. 708.

17. Golub, V.B., Chuvashov, A.V., Bondareva, V.V., et al., Results of Long-Term Observations on Stationary Transects in the Volga–Akhtuba Floodplain, *Biology Bulletin*, 2020, vol. 47, pp. 1309–1317.

18. Shi, L., Wang, Y., Jia, Y., Lu, C., Lei, G., and Wen, L., Vegetation Cover Dynamics and Resilience to Climatic and Hydrological Disturbances in Seasonal Floodplain: The Effects of Hydrological Connectivity, *Frontiers in Plant Science*, 2017, vol. 8, pp. 1–11.

19. Han, B., Benner, S.G., Bolte, J.P., et al., Coupling Biophysical Processes and Water Rights to Simulate Spatially Distributed Water Use in an Intensively Managed Hydrologic System, *Hydrol. Earth Syst. Sci.*, 2017, vol. 21, pp. 3671–3685.

20. Fernandes, L.F.S., Marques, M.J., Oliveira, P.C., and Moura, J.P., Decision Support Systems in Water Resources in the Demarcated Region of Douro – Case Study in Pinhao River Basin, Portugal, *Water Environ.*, 2019, vol. 33, pp. 350–357.

21. Weng, S.Q., Huang, G.H., and Li, Y.P., An Integrated Scenario-Based Multi-criteria Decision Support System for Water Resources Management and Planning – A Case Study in the Haihe River Basin, *Expert Syst. Appl.*, 2010, vol. 37, pp. 8242–8254.

22. McCord, J., Carron, J.C., Liu, B., Rhoton, S., et al., Pecos River Decision Support System: Application for Adjudication Settlement and River Operations EIS, *OpenSIUC*, 2004. URL: http://opensiuc.lib.siu.edu/ucowrconfs_2004/95?utm_source=o pensiuc.lib.siu.edu%2Fucowrconfs_2004%2F95&utm_medium =PDF&utm_campaign=PDFCoverPages.

23. Lam, F., Bolte, J., Santelmann, M., and Smith, C., Development and Evaluation of Multiple Objective Decision Making Methods for Watershed Management Planning, *J. Am. Water Resour. Assoc.*, 2002, vol. 38, pp. 517–529.

24. Misganaw, D., Guo, Y., Knapp, H.V., and Bhowmik, N.G., The Illinois River Decision Support System (ILRDSS), *Report Prepared for the Illinois Department of Natural Resources*, Illinois: Illinois State Water Survey, 1999.

25. Ge, Y., Li, X., Huang, C., and Nan, Z., A Decision Support System for Irrigation Water Allocation along the Middle Reaches of the Heihe River Basin, Northwest China, *Environmental Modelling & Software*, 2013, vol. 47, pp. 182–192.

26. Wriggers, P., Kultsova, M., Kapysh, A., et al., Intelligent Decision Support System for River Floodplain Management, *Communications in Computer and Information Science*, 2014, vol. 466, pp. 195–213.

27. O'Brien, G. and Wepener, V., Regional-Scale Risk Assessment Methodology Using the Relative Risk Model (RRM) for Surface Freshwater Aquatic Ecosystems in South Africa, *Water SA*, 2012, vol. 38, no. 2, pp. 153–165.

28. Tariq, M.A.U.R., Rajabi, Z., and Muttil, N., An Evaluation of Risk-Based Agricultural Land-Use Adjustments under a Flood Management Strategy in a Floodplain, *Hydrology*, 2021, vol. 8, no. 1, art. no. 53. DOI: 10.3390/hydrology8010053.

29. Lu, Y., Qin, F., Chang, Z., and Bao, S., Regional Ecological Risk Assessment in the Huai River Watershed during 2010–2015, *Sustainability*, 2017, vol. 9, no. 12, art. no. 2231.

30. Rincón, D., Velandia, J.F., Tsanis, I., and Khan, U.T., Stochastic Flood Risk Assessment under Climate Change Scenarios for Toronto, Canada Using CAPRA, *Water*, 2022, vol. 14, no. 2, art. no. 227. DOI: https://doi.org/10.3390/w14020227.

31. Modi, A., Kapoor, V., and Tare, V., River Space: A Hydro-Bio-Geomorphic Framework for Sustainable River-Floodplain Management, *Science of the Total Environment*, 2022, vol. 812. DOI: https://doi.org/10.1016/j.scitotenv.2021.151470.

32. *Scenarios and Indicators for Sustainable Development–Towards a Critical Assessment of Achievements and Challenges*, printed edition of the special issue published in *Sustainability*, Spangenberg, J.H., Ed., Basel: Multidisciplinary Digital Publishing Institute, 2019.

33. Ougolnitsky, G.A., Anopchenko, T.Yu., Gorbaneva, O.I., et al. Systems Methodology and Model Tools for Territorial Sustainable Management, *Advances in Systems Science and Applications*, 2018, vol. 18, no. 4, pp. 136–150.

34. Burkov, V.N., Novikov, D.A., and Shchepkin, A.V., *Control Mechanisms for Ecological-Economic Systems*, Cham: Springer, 2015.

35. Gorelits, O.V. and Zemlyanov, I.V., Current Flooding Mechanism for the Volga–Akhtuba Floodplain Areas During Floods (within the Volgograd Region), *Regional Scientific Potential at the Service of Modernization*, 2013, no. 2(5). (In Russian.)

36. Presnyakova, A.N., Pisarev, A.V., and Khrapov, S.S., The Flooding Dynamics of the Volga–Akhtuba Floodplain During Spring Flood Using Space Monitoring, *Science Journal of Volgograd State University. Mathematics. Physics*, 2017, no. 1 (38), pp. 66–74. (In Russian.)

37. Voronin, A., Khoperskov, A., Isaev, I., and Klikunova, A., Control Model of the Floodplain Territories Structure, *Adv. Syst. Sci. Appl.*, 2020, vol. 20, pp. 153–165.

38. Isaeva, I.I, Voronin, A.A., Khoperskov, A.V., and Kharitonov, M.A., Modeling the Territorial Structure Dynamics of the Northern Part of the Volga–Akhtuba Floodplain, *Computation*, 2022, vol. 10, no. 4. DOI: https://doi.org/10.3390/computation10040062.

39. Khrapov, S.S. and Khoperskov, A.V., Application of Graphics Processing Units for Self-Consistent Modelling of Shallow Water Dynamics and Sediment Transport, *Lobachevskii Journal of Mathematics*, 2020, vol. 41, no. 8, pp. 1475–1484.

40. Khrapov, S.S., Agafonnikova, E.O., Klikunova, A.Yu., et al., Numerical Modeling of Self-consistent Dynamics of Shallow Waters, Traction and Suspended Sediments: I. Influence of Commercial Sand Mining on the Safety of Navigation in the Channel of the Volga River, *Mathematical Physics and Computer Simulation*, 2022, vol. 25, no. 3, pp. 31–57. DOI: https://doi.org/10.15688/mpcm.jvolsu.2022.3.3. (In Russian.)

41. Khrapov, S.S., Numerical Modeling of Self-consistent Dynamics of Shallow and Ground Waters, *Mathematical Physics and Computer Simulation*, 2021, vol. 24, no. 3, pp. 45–62. DOI: https://doi.org/10.15688/mpcm.jvolsu.2021.3.5. (In Russian.)

42. Khrapov, S.S., Numerical Modeling of Hydrodynamic Accidents: Erosion of Dams and Flooding of Territories, *Vestnik of Saint Petersburg University. Mathematics. Mechanics. Astronomy*, 2023, vol. 10, no. 2, pp. 357–373. https://doi.org/10.21638/spbu01.2023.215. (In Russian.)

43. Klikunova, A.Yu. and Khoperskov, A.V., Creation of Digital Elevation Models for River Floodplains, *CEUR Workshop Proceedings*, 2019, vol. 2391, pp. 275–284.

44. Klikunova, A.Yu. and Khoperskov, A.V., Numerical Hydrodynamic Model of the Lower Volga, *Journal of Physics: Conference Series*, 2018, vol. 1128, art. no. 012087. DOI: https://doi.org/10.1088/1742-6596/1128/1/012087.

45. Khrapov, S.S., Khoperskov, A.V., and Kuz'min, N.M., A Numerical Scheme for Simulating the Dynamics of Surface Water

on the Basis of the Combined SPH-TVD Approach, *Numerical Methods and Programming*, 2011, vol. 12, pp. 282–297. (In Russian.)

46. Khrapov, S., Pisarev, A., Kobelev, I., et. al., The Numerical Simulation of Shallow Water: Estimation of the Roughness Coefficient on the Flood Stage, *Advances in Mechanical Engineering*, 2013, vol. 2013, art. ID 787016.

47. Dyakonova, T., Khoperskov, A., and Khrapov, S., Numerical Model of Shallow Water: The Use of NVIDIA CUDA Graphics Processors, *Communications in Computer and Information Science*, 2016, vol. 687, pp. 132–145.

48. Voronin, A.A., Eliseeva, M.V., Pisarev, A.V., et al., Simulation Models of Surface Water Dynamics Using Remote Sensing Data: Effect of Terrain, *The Caspian Journal: Control and High Technologies*, 2012, no. 3 (19), pp. 54–62. (In Russian.)

49. Voronin, A., Vasilchenko, A., and Khoperskov, A., Project Optimization for Small Watercourses Restoration in the Northern Part of the Volga–Akhtuba Floodplain by the Geoinformation and Hydrodynamic Modeling, *Journal of Physics: Conf. Series*, 2018, vol. 973, pp. 1–10. URL: http://iopscience.iop.org/article/10.1088/1742-6596/973/1/012064/pdf.

Author information

Isaeva, Inessa Igorevna. Junior Researcher, Volgograd State University, Volgograd, Russia
✉ isaeva-inessa@mail.ru
ORCID iD: https://orcid.org/0000-0003-3045-6757

Kharitonov, Mikhail Alekseevich. Cand. Sci. (Eng.), Volgograd State University, Volgograd, Russia
✉ kharitonov@volsu.ru
ORCID iD: https://orcid.org/0000-0002-2115-1591

Vasilchenko, Anna Anatol'evna. Cand. Sci. (Eng.), Volgograd State University, Volgograd, Russia
✉ aa-vasilchenko@mail.ru
ORCID iD: https://orcid.org/0000-0003-4945-9552

Voronin, Alexander Alexandrovich. Dr. Sci. (Phys.–Math.), Volgograd State University, Volgograd, Russia
✉ voronin.prof@gmail.com
ORCID iD: https://orcid.org/0000-0001-7912-9963

Khoperskov, Alexander Valentinovich. Dr. Sci. (Phys.–Math.), Volgograd State University, Volgograd, Russia
✉ khoperskov@volsu.ru
ORCID iD: https://orcid.org/0000-0003-0149-7947

Agafonnikova, Ekaterina Olegovna. Associate Professor, Volgograd State University, Volgograd, Russia
✉ agafonnikova@volsu.ru
ORCID iD: https://orcid.org/0000-0002-2862-4531

Cite this paper